

The Effect of Pull Speed and Heat Treatment on Thermal Donors in Czochralski Silicon

Espen Olsen, Torbjørn Mehl, Helene Eikaas Stalheim, Mari Juel, Rune Søndenå, and Ingunn Burud*

In silicon crystals manufactured by the Czochralski method, oxygen is incorporated as a contaminant originating primarily from dissolution of the quartz crucible used to contain the molten silicon feedstock. The oxygen can be found either as interstitials, agglomerates, or as oxide particles. Particular kinds of agglomerates are known to lead to the formation of thermal donors—electronic states in the bandgap of the silicon base material. These can act as sites for recombination of excited charge carriers and are called thermal donors due to their ability to inject two electrons into the conduction band of silicon by thermal excitation, leading to enhanced electrical conductivity. Neither of these features are desirable in Cz-Si manufacture. Herein, the behavior of thermal donors as a function of the pull speed, and the position in the ingot, is investigated. Thermal treatment is provided, first for the formation of thermal donors and then for their removal. The aim is to investigate methods for minimizing their incorporation in the crystal in the first place and then how they can be removed. Hyperspectral imaging and spectroscopy combined with Fourier-transform infrared spectroscopy are used.

1. Introduction

Czochralski-grown silicon wafers (Cz-Si) are the main sources of materials for high-performance silicon solar cells today. As more advanced techniques for processing the wafers into solar cells are used, the need to have complete control over the material

E. Olsen, T. Mehl, H. E. Stalheim, I. Burud
 Faculty of Science and Technology Department of Physics
 Norwegian University of Life Sciences (NMBU)
 Universitetstunet 3, Ås 1432, Norway
 E-mail: espen.olsen@nmbu.no

M. Juel
 Department for Sustainable Energy Technology
 SINTEF Industry
 P.O. Box 4760 Torgarden, Trondheim N-7465, Norway

R. Søndenå
 Department for Solar Energy
 Institute for Energy Technology
 P.O. Box 40, Kjeller N-2027, Norway

 The ORCID identification number(s) for the author(s) of this article can be found under <https://doi.org/10.1002/pssa.202100655>.

© 2021 The Authors. physica status solidi (a) applications and materials science published by Wiley-VCH GmbH. This is an open access article under the terms of the Creative Commons Attribution License, which permits use, distribution and reproduction in any medium, provided the original work is properly cited.

DOI: [10.1002/pssa.202100655](https://doi.org/10.1002/pssa.202100655)

properties are becoming ever more important. Impurities are always present to a certain degree, originating from the feedstock polysilicon, crystal-growing equipment, and, most importantly, from the quartz crucibles used for containing the molten silicon feedstock. Metallic impurities such as Fe, Al, and Cr are considered detrimental if present in more than trace amounts due to their ability to form states in the bandgap, leading to increased recombination of photogenerated charge carriers via the Shockley–Read–Hall (SRH) mechanism. Oxygen is an element introduced to the grown crystal primarily from the quartz crucible consisting of silica (SiO_2). Oxygen is a small atom primarily present interstitially as O_i ; however, small and large agglomerates as well as oxide particles frequently exist in the structure. The distribution of oxygen in Cz-Si ingots is governed by complex processes involving the shape of the diffusion layer on the solidifying front as well as the content of O in the molten feedstock. This is controlled by dissolution of material from the crucible wall. The rotation speed of both the crucible and the ingot has significant impact on the transport of O from the wall to the solidifying surface. Incorporation of small amounts of oxygen is not considered as harmful as it normally will occur as interstitial oxygen. These are referred to not forming states in the bandgap, leading to SRH recombination, and are considered electrically inactive.^[1–4] However, larger amounts will be detrimental as supersaturation may lead to formation of electrically active agglomerates and particles. It was found in 1957 that by heating oxygen-rich silicon up to 450 °C, electrically active defects were generated, later called thermal donors (TDs).^[1,5] Since then, numerous researchers have been trying to elucidate the detailed behavior of TDs. 60 years later, the details of the processes by which the defects are generated and eliminated are not completely clear. However, several authors^[6–8] and most recent^[9–11] have studied the phenomenon. A comprehensive review on diffusion mechanisms of oxygen in silicon has been published.^[7] Reports are made on evidence of a mechanism where interstitial oxygen is able to move through the Si lattice at 450 °C and form clusters of individual atoms at voids and other crystal faults. These introduce states in the bandgap and act as double donors to the conduction band with the ability to be thermally excited. This leads to decreased resistivity and possible recombination. This is

considered undesirable as it involves loss of process control and possible loss of solar cell efficiency.

TD clusters have been reported to form a number of complexes with a varying number of atoms introducing several states in the bandgap. Matsushita^[12] found that the point defect density increases exponentially as the temperature in the annealing process decreases; hence, a dependence is found during crystal growth. The density of point defects differs from one position in the ingot to another, even though the initial oxygen concentration is the same. This means that the formation of point defects not only depends on oxygen concentration, but also on thermal history during crystal growth.^[12] The seed end will stay in the cold zone of the Cz-Si pulling process for a prolonged time, and the thermal history will thereby vary as a function of crystal height with deviations in impurity distribution. A study by Nakanishi et al.^[13] showed that if different cooling profiles are used for two crystals, the fastest cooling crystal will have less supersaturated oxygen precipitates after 12 h heat treatment. When the crystal grows and solidifies, the oxygen out-diffuses and there is a drastic decrease in oxygen concentration in Cz material near the periphery region. Several authors^[14–17] have shown that the defects created by interstitial oxygen and other impurities are distributed in a swirl, ring-like pattern in horizontally cut wafers. This has also recently been studied by our group.^[18] The spatial distribution of the rings can thus be connected directly to the concentration of oxygen in the lattice. If the material is thermally annealed at 450 °C, the distribution of the ring pattern changes and increased TD concentrations are observed which can be measured as increase in conductivity.^[1] We previously reported on hyperspectral imaging to study the effects of heat treatment on the formation of TDs in as-cut Cz-Si wafers.^[18] The associated spectral and spatial characteristics of luminescence emitted after photoexcitation of electrons by 808 nm laser light were recorded. In these works, a characteristic and complex spectral signature was found, involving several separate emission lines, including what has been denoted as the P-and H-lines in previous work by Minaev and Mudryi.^[19] Such a spectrum is shown in **Figure 1**, while the details for each line are shown in **Table 1**. The emissions were recorded after the

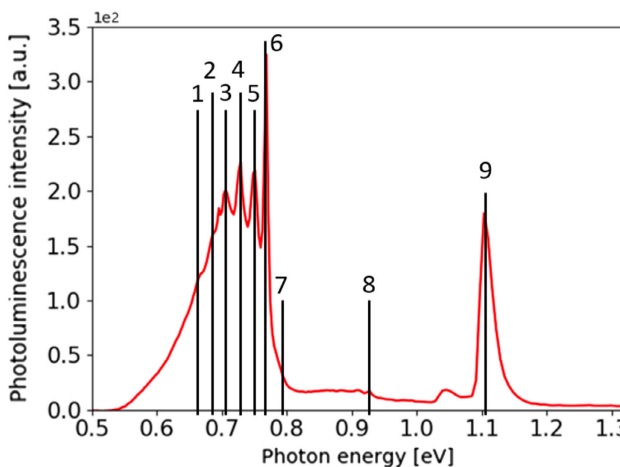


Figure 1. Overview of the spectral emission lines found in Cz-Si exhibiting TDs.^[18–20] Details of each of the emission lines are shown in **Table 1**.

Table 1. Details for the separate emission lines as shown in **Figure 1**. Luminescence via the intrinsic, direct band-to-band recombination mechanism at 1.12 eV is denoted BB.

| Spectral line in Figure 1 | Name | Lower integration limit | Higher integration limit | Peak [eV] |
|------------------------------|---------|----------------------------|-----------------------------|-----------|
| 1 | 0.67 eV | 0.66 | 0.68 | 0.667 |
| 2 | 0.68 eV | 0.68 | 0.69 | 0.685 |
| 3 | 0.70 eV | 0.70 | 0.71 | 0.705 |
| 4 | 0.72 eV | 0.72 | 0.73 | 0.725 |
| 5 | 0.75 eV | 0.74 | 0.75 | 0.749 |
| 6 | P-line | 0.76 | 0.77 | 0.767 |
| 7 | C-line | 0.78 | 0.79 | 0.789 |
| 8 | H-line | 0.92 | 0.93 | 0.925 |
| 9 | BB | 1.08 | 1.15 | 1.12 |

samples were annealed at 450 °C for up to 99 h. The signal grew with time at the elevated temperature. This was attributed to TDs which enabled studies of the spatial distribution in the wafers. When treated at 650 °C, the complex spectrum was replaced by a simpler, broad emission without the characteristic emission lines. A broadband emission with similar characteristics has been attributed to carbon (C-line).^[20]

In the Cz-Si growing process, the upper, cooling part of the ingot can be exposed to temperatures able to induce the formation of TDs. As Cz-Si wafers exhibiting TDs are not considered as prime grade for high-efficiency solar cells without individual, further treatment, this will represent a loss for the manufacturer. As the formation and behavior of TDs is not fully understood, insight is needed to further enhance the manufacturing process. In the present work, the effect of TDs will be studied as a function of the height in two crystals pulled at different speeds. Characterization will be carried out by hyperspectral photoluminescence (HSPL) imaging of etched and unetched Cz-Si cross-section samples. Complementary characterization will be performed by Fourier-transform infrared spectroscopy (FTIR). The samples are studied before and after thermal annealing at 450 °C and at 650 °C.

2. Experimental Section

The samples used in this study were slabs cut vertically from two different n-type (p-doped, 1–3 ohm cm) Cz-Si ingots of 1100 mm

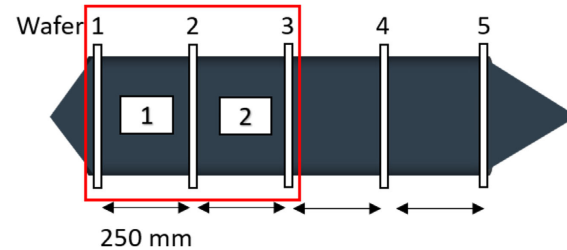


Figure 2. Partitioning of the ingots. Five conventional, horizontally cut slabs were cut between the segments. Two segments (one and two) were used for further study.

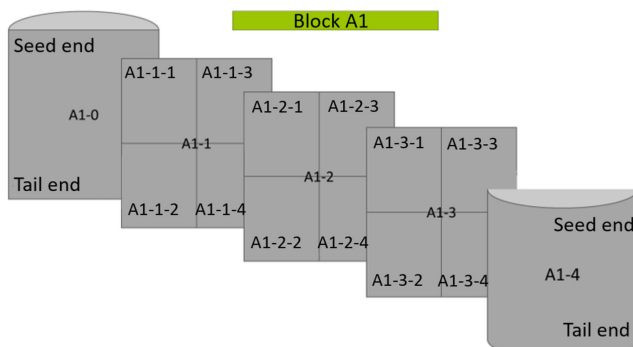


Figure 3. The partitioning of the segments with designation marks as applied to segment A1. The samples marked A1-2-1 (etched) and A1-3-1 (unetched) were studied by HSPL, while the segment A1-2-3 positioned directly oppositely in the pull direction was studied by FTIR for mapping of O_i .

length and 203 mm diameter. The pull speed was 0.9 and 1.3 mm min⁻¹ in ingot A and ingot B, respectively. The top and tail were removed and the ingot was further cut into four segments of \approx 250 mm length. The partitioning of the ingots is sketched in **Figure 2**.

The two topmost segments (toward the seed end) were chosen for further study. Three centrally positioned slabs of 2.65 mm thickness were cut vertically from each segment according to **Figure 3**. These centrally positioned slabs were further divided into four samples, each now with dimensions ($l \times w$) 125.3 mm \times 102.5 mm. The samples were marked individually according to **Figure 3**. The samples studied by HSPL were marked A1-2-1 (etched) and A1-3-1 (unetched) in **Figure 3**. The slabs on the opposite side, for example, A1-2-3, were studied by FTIR to determine the content of O_i . Due to radial symmetry of the oxygen distribution, FTIR measurements at a set height and radial position should be representative for the samples used for HSPL as well. For simplicity, the samples studied by HSPL are hereafter denoted A1 and A2 from ingot A and B1 and B2 from ingot B, respectively.

To remove saw damage to the surfaces, one set of samples were etched in a HNA solution, that is, hydrofluoric acid, nitric acid, and acetic acid (2:10:5) for 10 min at 75 °C. This was not fully successful and a second etch was performed, also in a new HNA etch but now at 25–35 °C, again for 10 min, resulting in a visible smooth surface. This removed 0.2 mm of material, giving a final thickness of the samples of 2.45 mm. Another set of samples were kept as cut (unetched) and were not chemically polished before examination with HSPL.

For measurement of the content of O_i as a function of height in the crystal, FTIR was performed on the so-designated samples. Measurements were made from top to bottom, 10, 20, and 90 mm from the center of the ingot for sample A and 10 and 90 mm from the center of the ingot for sample B. The measurements were made for every 10 mm by a Thermo Nicolet 6700 FTIR running the OMNIC software using the standard SEMI MF1188-1107 for quantification of interstitial oxygen.

HSPL (explained below) was performed before heat treatment on the etched and unetched samples designated for this.

To remove possible organic contaminants, the samples were rinsed with Piranha solution ($H_2SO_4:H_2O_2$, ratio 4:1) at 115–120 °C for 8 min. A subsequent dip in a 5% HF solution removed the chemical oxide prior to the heat treatment. All (both etched and unetched) samples were heat treated at 450 °C for 66 h flushed with N_2 (grade 5.0, AGA) in a Tempress quartz furnace. HSPL was again performed on the thermally treated samples. The samples were then heat treated at 650 °C for 1 h in the same furnace as described earlier after a similar cleaning procedure with Piranha solution with subsequent rinsing. A final investigation by HSPL was then performed.

A detailed description of the setup for HSPL can be found in the referenced literature.^[18,21,22] However, a brief description follows. A hyperspectral linescan pushbroom camera (Specim SWIR, Uolu, Finland) equipped with a MCT detector with sensitivity for photons in the 0.490–1.334 eV range (2500–930 nm) was used. The resolution used in these investigations (pixel size) was 343 μ m; however, this was adjustable down to about 20 μ m depending on the setup. Photoexcitation was performed by a 808 nm (1.53 eV) line laser (Coherent, Lasiris Magnum II, Gammadata AB, Kiruna, Sweden). The average penetration depth in silicon of the photoexciting light at 90 K was 67 μ m. The irradiated density was 2 W cm⁻². The samples were cooled to 90 K by placing them on a liquid nitrogen (LN_2)-cooled sample holder with polished aluminum surface. The temperature was monitored by a thermocouple type T in direct contact with the holder. The setup is depicted in **Figure 4**.

3. Results and Discussion

3.1. Oxygen Measurements

The results from the FTIR measurements regarding the levels of interstitial oxygen O_i in the material are shown in **Figure 5**.

Ingot A exhibited more O_i than ingot B, the difference is more pronounced further down in the ingot from the seed end than at

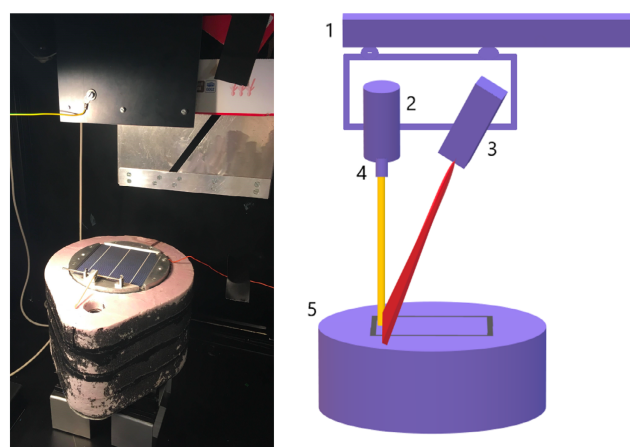


Figure 4. HSPL setup. An 808 nm line laser (3) illuminates the sample while a hyperspectral line scan camera (2) is used for imaging. The sample is placed on the cryogenic holder (5) and scanned by moving the combined camera/laser over the sample holder with a linear translation stage (1). A long-pass filter (4) prevents reflected laser light to enter the camera.

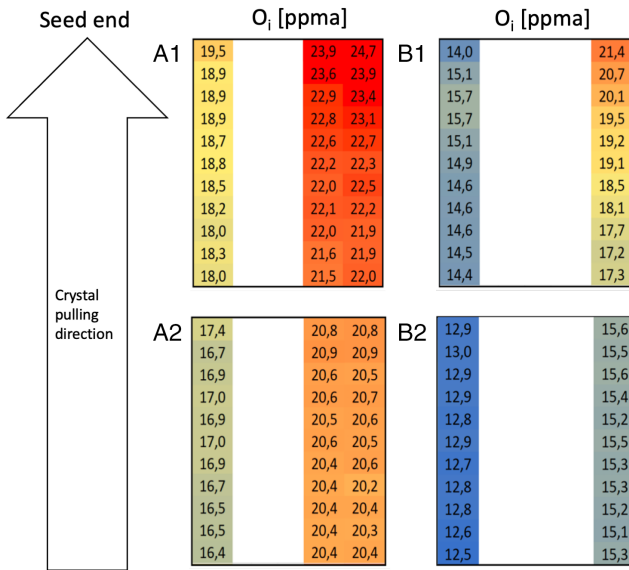


Figure 5. The content of interstitial oxygen O_i in the samples as measured by FTIR. The pull speed of ingot A was 0.9 mm min⁻¹ and ingot B was 1.3 mm min⁻¹.

the top. Further, the samples nearest to the seed end have the highest levels. O_i is as expected depleted toward the edge of the crystal compared with the center. It is interesting to note that the B2 sample exhibits O_i levels below those reported to form measurable levels of TDs in Cz-Si.^[23]

3.2. PL Spectra: Response upon Thermal Annealing

The integrated (from the whole sample) PL spectra recorded by HSPL at 90 K from the etched, chemically polished sample set are shown in **Figure 6** and 7, while the integrated spectra from the as-cut, unetched samples are shown in **Figure 8** and 9. The samples after 450 °C thermal treatment are marked as TD dominated, while the samples after treatment at 650 °C are marked as TD free.

Figure 6 shows that, after production, the slowly pulled (0.9 mm min⁻¹) sample A1, closest to the seed end, exhibited a strong, characteristic signal in the 0.6–0.8 eV range attributable to TDs.^[18] This signal is of similar strength as the signal due to the direct band-to-band transition at 1.1 eV. Thermal treatment at 450 °C did not change this signal's strength significantly, suggesting that TD formation was almost completed in the pulling process. However, the Band-to-band (BB) signal was reduced,

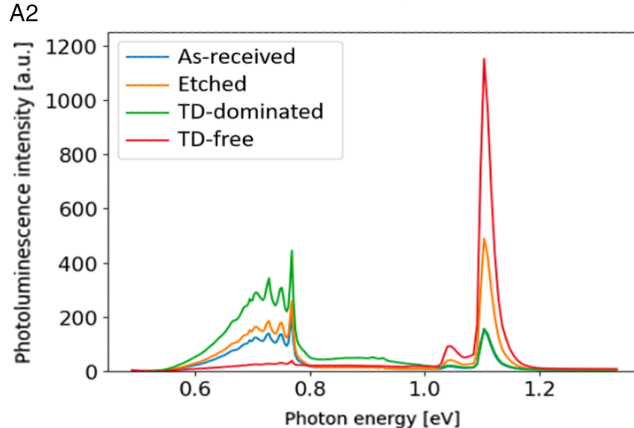
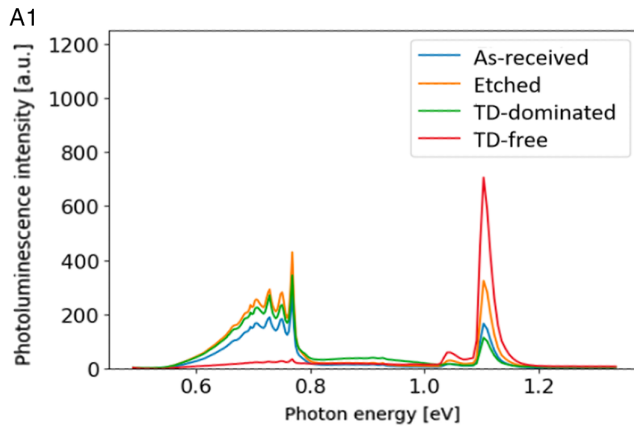


Figure 6. The PL spectra from the etched samples A1 and A2 at 90 K before and after thermal treatment. TD dominated: 450 °C/66 h. TD free: 650 °C/1 h.

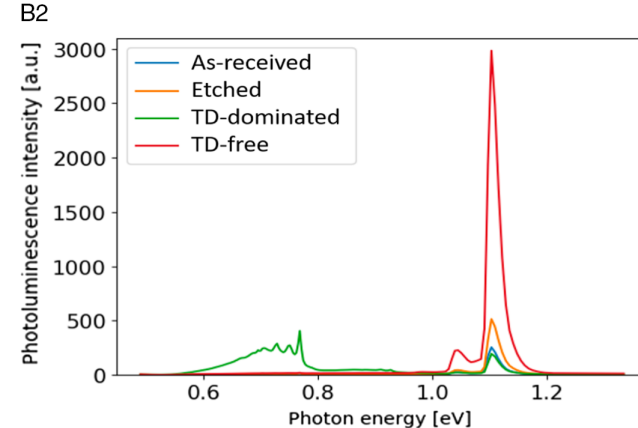
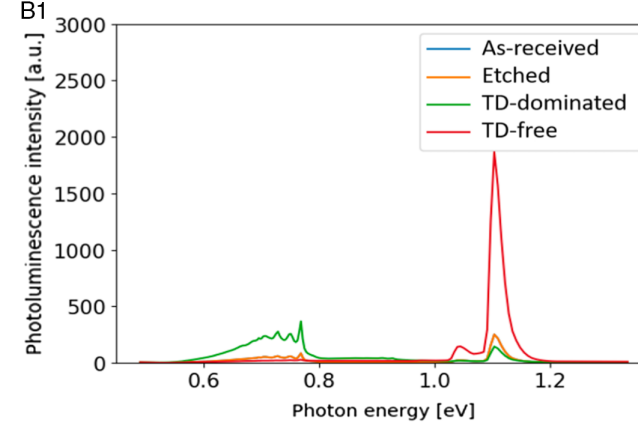


Figure 7. The PL spectra from the etched samples B1 and B2 at 90 K before and after thermal treatment. TD dominated: 450 °C/66 h. TD free: 650 °C/1 h.

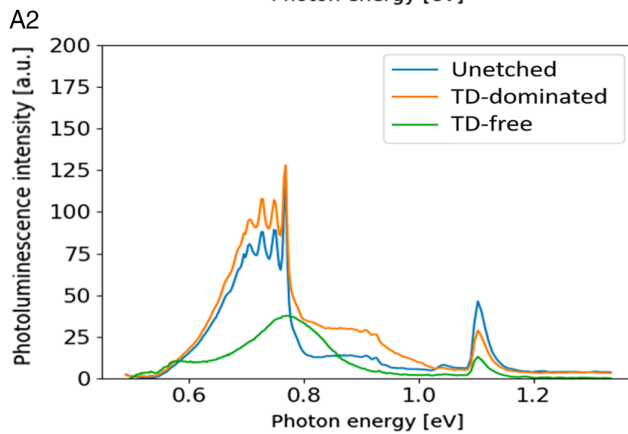
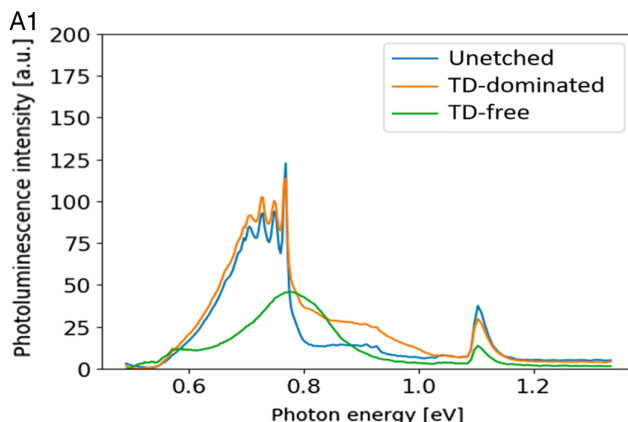


Figure 8. The PL spectra from the unetched samples A1 and A2 before and after thermal treatment. TD dominated: 450 °C/66 h. TD free: 650 °C/1 h.

indicating more SRH recombination. Exposure to 650 °C for 1 h almost suppressed the 0.6–0.8 eV signal completely and considerably enhanced the BB signal, suggesting a significant decrease in SRH recombination and thereby also an increase in photogenerated charge carrier lifetime. Sample A2 exhibited TD-related luminescence also in the as-received state, but in this case thermal treatment at 450 °C enhanced this signal considerably, suggesting that additional TDs formed during the anneal. Again, exposure to 650 °C for 1 h almost eliminated this signal and gave a strongly enhanced BB signal.

The spectral response of the more rapidly pulled sample set (B1 and B2, 1.3 mm min⁻¹) shown in Figure 7 is quite different. After production, the seed end sample (B1) only exhibits a very minor emission signal in the 0.6–0.8 eV range attributable to TDs. Treatment at 450 °C results in the appearance of this signal to similar levels, as found in the slowly pulled sample A. Anneal at 650 °C almost completely removes the TD signal and again the direct BB signal is strongly enhanced. Untreated, the sample B2, further down in the ingot, does not exhibit detectable emissions attributable to TDs. Thermal treatment at 450 °C again brings forth the characteristic emission spectrum attributable to TDs at similar levels as in the other samples, while at the same time reducing the BB emission, indicating enhanced SRH recombination. Treatment at 650 °C completely removes the 0.6–0.8 eV signal and a strongly enhanced BB PL signal can again be noted—an

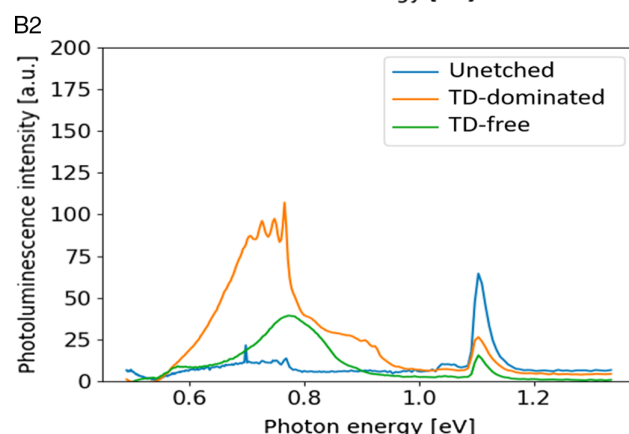
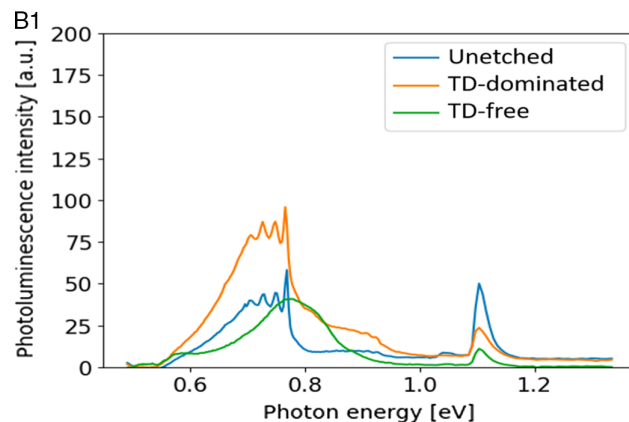


Figure 9. The PL spectra from the unetched samples B1 and B2 before and after thermal treatment. TD dominated: 450 °C/66 h. TD free: 650 °C/1 h.

indication that SRH recombination is strongly reduced, resulting in a higher lifetime of photogenerated charge carriers at 90 K.

The PL spectra from the unetched seed end sample of the slowly pulled crystal are shown in Figure 8. These samples have a rough, as-cut surface, which is supposed to exhibit very high surface recombination. Previous works have shown this to be detrimental to the signal from band-to-band recombination over the indirect bandgap of Si in cooled samples due to few phonons being available at cryogenic conditions, enabling charge carriers to diffuse to the surfaces.^[18]

This results in lower injection levels during measurements, potentially affecting the signals from rapid, bulk SRH recombination processes, albeit to a much lower degree. The rough surface may also contribute to higher absorption of exciting radiation near the surface, as well as scattering effects, all contributing to lower injection levels in such samples. With the abovementioned considerations in mind, the materials from both the A and B ingots follow the behavior as found for the etched samples with low surface roughness. An interesting deviation is found for all the samples after the treatment at 650 °C. In a previous study on conventional as-cut, unpassivated Cz-Si wafers, we^[18,24] found that treatment at 650 °C for 1 h removed the characteristic spectrum attributable to TDs and led to the appearance of a broad peak with center energy around the P line (0.767 eV), while at the same time almost killing the BB signal

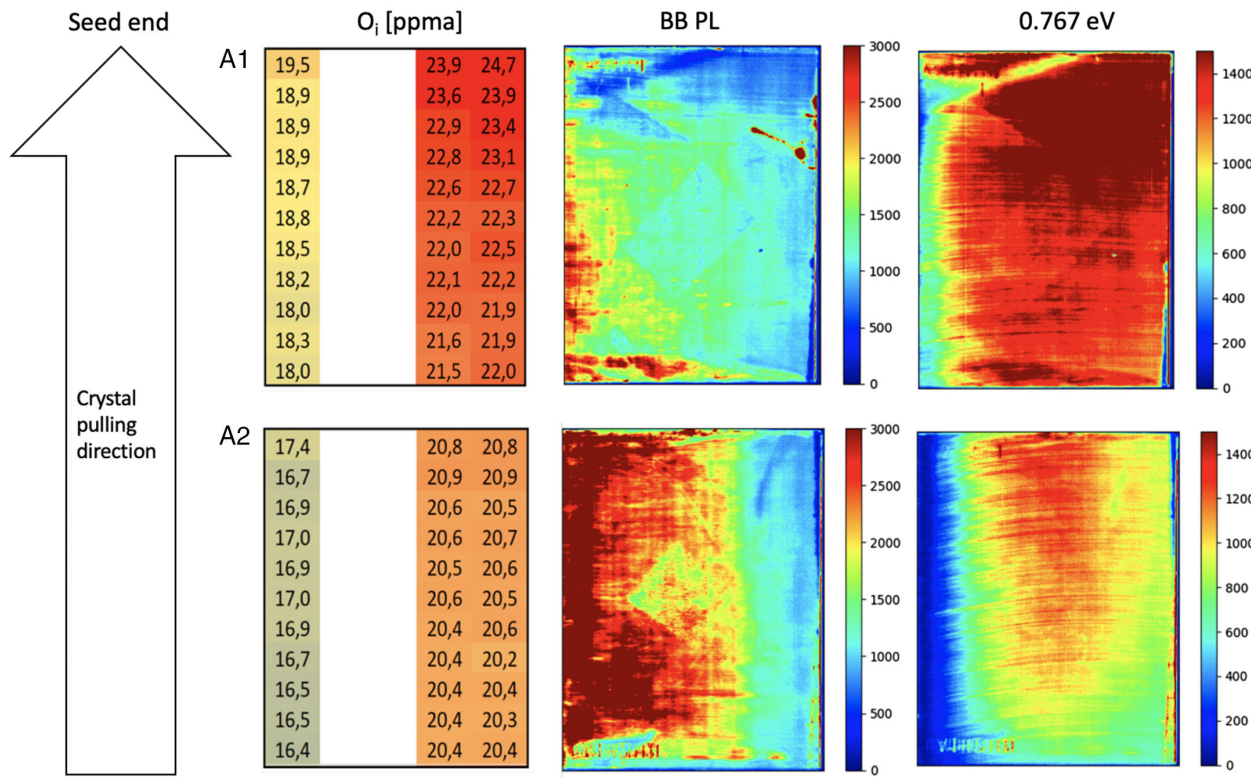


Figure 10. The distribution of the BB PL (1.12 eV) and the TD-attributed (0.767 eV) signals in the vertically cut, etched samples from ingot A (0.9 mm h^{-1}). The corresponding content of O_i measured by FTIR is included for comparison.

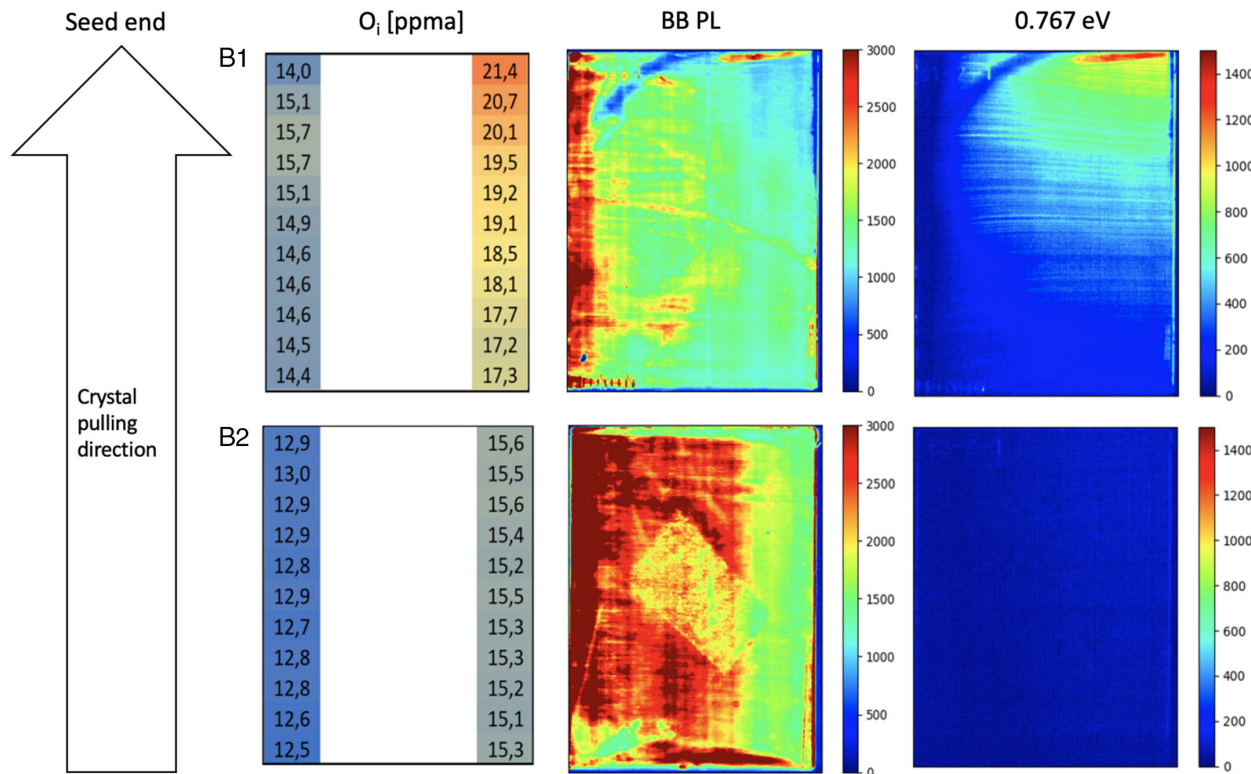


Figure 11. The distribution of the BB PL (1.12 eV) and the TD-attributed (0.767 eV) signals in the vertically cut, etched samples from ingot B (1.3 mm h^{-1}). The corresponding content of O_i measured by FTIR is included for comparison.

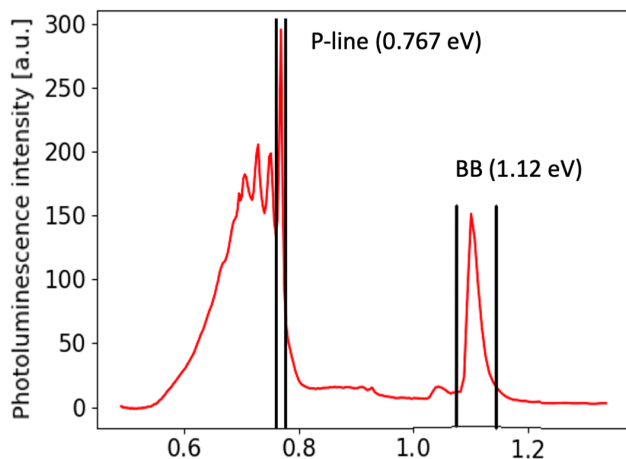


Figure 12. The integration limits for the signals depicted spatially in Figure 10–13.

and so the lifetime of charge carriers effectively. The same feature is clearly found in the unetched samples in this study. This signal was not found with the etched samples (Figure 6 and 7). This leads to the interesting conclusion that this is a surface effect. Radiative surface recombination has to our knowledge

not been reported before. This remains an interesting topic for further studies. It is well known that at temperatures above 650 °C, TD-forming oxygen clusters disappear from the structure by fast diffusion to form oxide particles.^[7] A broad emission with center energy 0.78 eV has in several studies been linked to carbon in bulk monocrystalline silicon materials.^[20] However, this is not consistent with our recordings of this as a surface effect. As the low-signal strengths resulted in low Signal to noise ratio (S/N) ratio for spatial images, the unetched samples are not treated further here.

3.3. Spatial Distribution of PL Emissions in the Etched Samples before Thermal Treatment

Images of the spatial distribution of the band-to-band- (1.12 eV) and TD-associated (0.767 eV) PL signals coupled with the O_i measurements are shown in Figure 10 and 11. Figure 12 depicts the spectral integration limits used for the BB- and P-line (0.767 eV) signals, respectively. As the other TD-associated emission lines shown in Table 1 (0.67–0.72 eV) follow the P-line at 0.767 eV, focus will be put on the P-line emission.

In general, the materials behave as expected given their different pulling speed. Crystal A contains more O_i than the faster pulled crystal B. The band-to-band luminescence signal, associated with higher lifetimes of charge carriers, is of similar

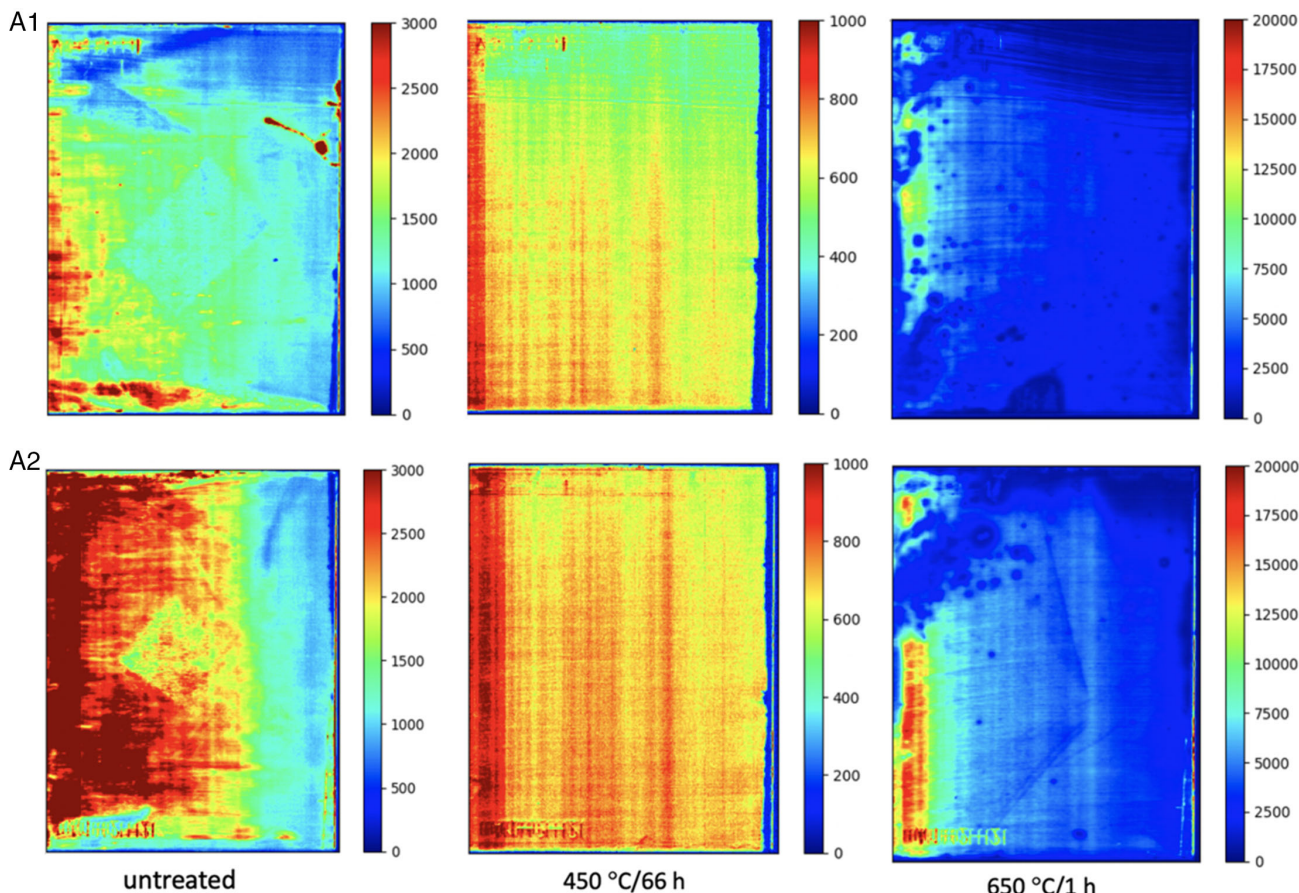


Figure 13. The development in the spatial distribution of the BB (1.12 eV) PL emission in crystal A (0.9 mm min^{-1}) before and after thermal treatment at 450 and 650 °C.

magnitude and distribution. Sample A1 and B1 close to the seed end exhibit less BB PL than sample A2 and B2 closer to the tail end. The striation lines from the pulling are clearly visible. These are formed during pulling by slight variations in the growth rate and diffusion of oxygen and dopants through the solidification boundary as pulling conditions are constantly adjusted. In conventional, horizontal cut wafers, these are the causes of ring-like structures reported in other studies.^[25,26] A square-like artifact in the middle of A2 or B2 is likely to be attributed to higher surface recombination from organic deposits from a paper division sheet during transport. As shown in the figures in Section 3.4, this feature disappeared after treatment with Piranha solution prior to heat treatment. BB PL is considerably enhanced toward the edge of the ingot compared with the center part. This is in line with the content of O_i as the ingot periphery is depleted of oxygen. Indications of the transitions in the ingots from self-interstitial-dominated to vacancy-dominated zones (P-band) also reported by others^[27,28] can be seen in the upper-left corner of the seed-end samples in both ingots. This interstitial- and vacancy-free transition area is supposed to be a dense area in the crystal with low diffusivity for oxygen. This feature is also evident by a reduced TD-attributed signal at 0.767 eV. This TD signal is quite different between the two ingots. Ingot A is dominated by this, showing a visible gradient

with distance from the seed. This reflects the considerations made in Section 3.2, where the slowly pulled ingot exhibited large amounts of PL attributable to TDs, which seemed to fully have formed in this sample during crystal pulling. Heat treatment at 450 °C did not lead to further enhancement of this signal. The A2 sample farther from the seed end shows considerably lower PL emissions from TDs, in particular toward the edge, where the content of O_i is less than that toward the middle. The seed end sample B1 from ingot B shows some signal attributable to TDs only in the topmost parts where the content of O_i is the largest. B2 sample from ingot B seemingly does not emit this signal at all, supporting previous reports of a threshold value for the onset of formation of TDs.^[23]

3.4. Spatial Distribution and Development of the BB (1.12 eV) and P-Line (0.767 eV) Emissions Upon Heat Treatment

Images of the spatial distribution of the band-to-band PL emission for the samples before and after heat treatment are shown in Figure 13 and 14. Corresponding images of the P-line (0.767 eV) emission are shown in Figure 15 and 16.

The band-to-band emission behaves quite similarly in all the samples for both ingots, before heat treatment. The seed end

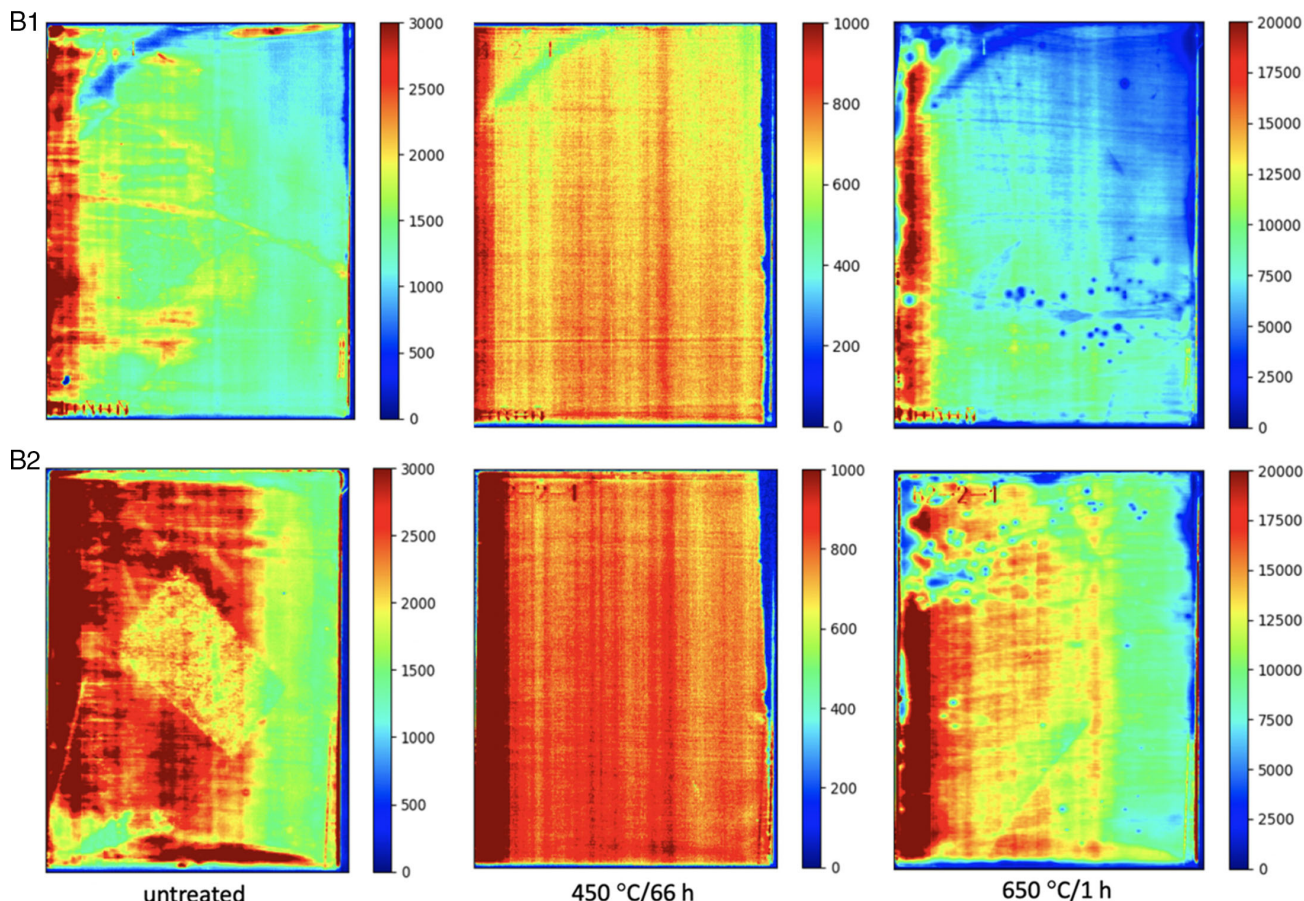


Figure 14. The development in the spatial distribution of the BB (1.12 eV) PL emission in crystal B (1.3 mm min⁻¹) before and after thermal treatment at 450 and 650 °C.

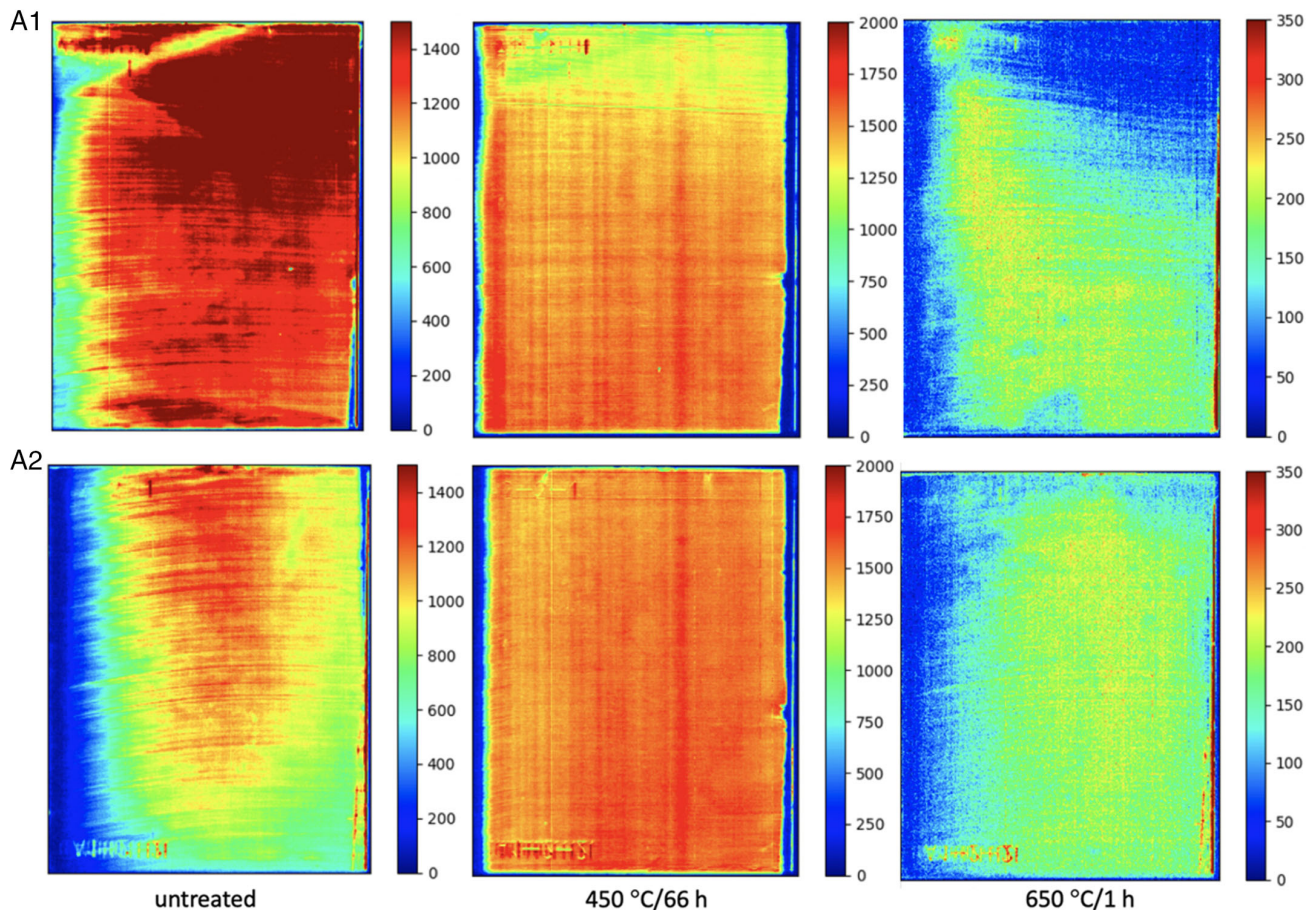


Figure 15. The development in the spatial distribution of the P-line (0.767 eV) PL emission in crystal A (0.9 mm min^{-1}) before and after thermal treatment at 450 and $650\text{ }^\circ\text{C}$.

sample exhibited a substantial less BB PL, except at the periphery of the ingot, where the content of O_i is lower than that in the center. Thus, a high BB signal is often seen toward the outer edge of the crystal. After TD formation at $450\text{ }^\circ\text{C}$, the BB PL is evened out over the samples as the individual features of the good areas disappear in the image and the whole sample, except for the top seed end part and the very periphery, luminescence at an even and substantially lower intensity. This is reflected in the spectra shown in Figure 6. After treatment at $650\text{ }^\circ\text{C}$, individual high- and low-lifetime areas reappear, and a significantly stronger BB signal is in general obtained. A notable exception is the top, center part of the seed end ingot A, where the BB PL is of similar magnitude as in the untreated sample.

The distribution of the P-line emission at 0.767 eV is substantially different between the two ingots. This emission line can be attributed to TDs linked to oxygen clusters and as the two ingots were manufactured to exhibit differences in the oxygen level, this is as expected. Comments on the untreated samples, which show strikingly different distributions of this signal, can be found in Section 3.3. The samples from both ingots respond similarly to TD formation treatment at $450\text{ }^\circ\text{C}$. The P-line signal appears evenly distributed in the samples after thermal anneal, except for in the very peripheral, oxygen-depleted part of the ingot where it is absent. This supports the results from a previous study^[18]

where conventional Cz-Si wafers were exposed to the same treatment as here. Oxygen-related striation marks from the pulling are clearly evident, particularly in ingot B with the least O_i content. Sample A1 with the highest O_i content shows less signal toward the seed end. This is difficult to explain but can be caused by excessive diffusion upon prolonged heat exposure and growth of even larger oxygen precipitates, that are not TDs. Haunschild et al. previously demonstrated the presence of black cores/black hearts in Cz-Si wafers caused by oxygen agglomeration.^[29] The low BB signal certainly indicates the presence of lifetime-limiting impurities, most likely oxygen. Oxygen precipitates themselves are mainly electrically inactive but their growing size might cause strain in the silicon lattice affecting the lifetime negatively.^[30] The treatment at $650\text{ }^\circ\text{C}$ seemingly deactivates the recombination processes associated with the P-line emission in all the samples. The signal is still present but at very low intensities. Again, sample A1 shows very low levels of this signal in the top, center part, toward the seed end of the ingot.

4. Summary and Conclusion

HSPL imaging gives the ability to record images with high-resolution emission spectra covering a large span of wavelengths.

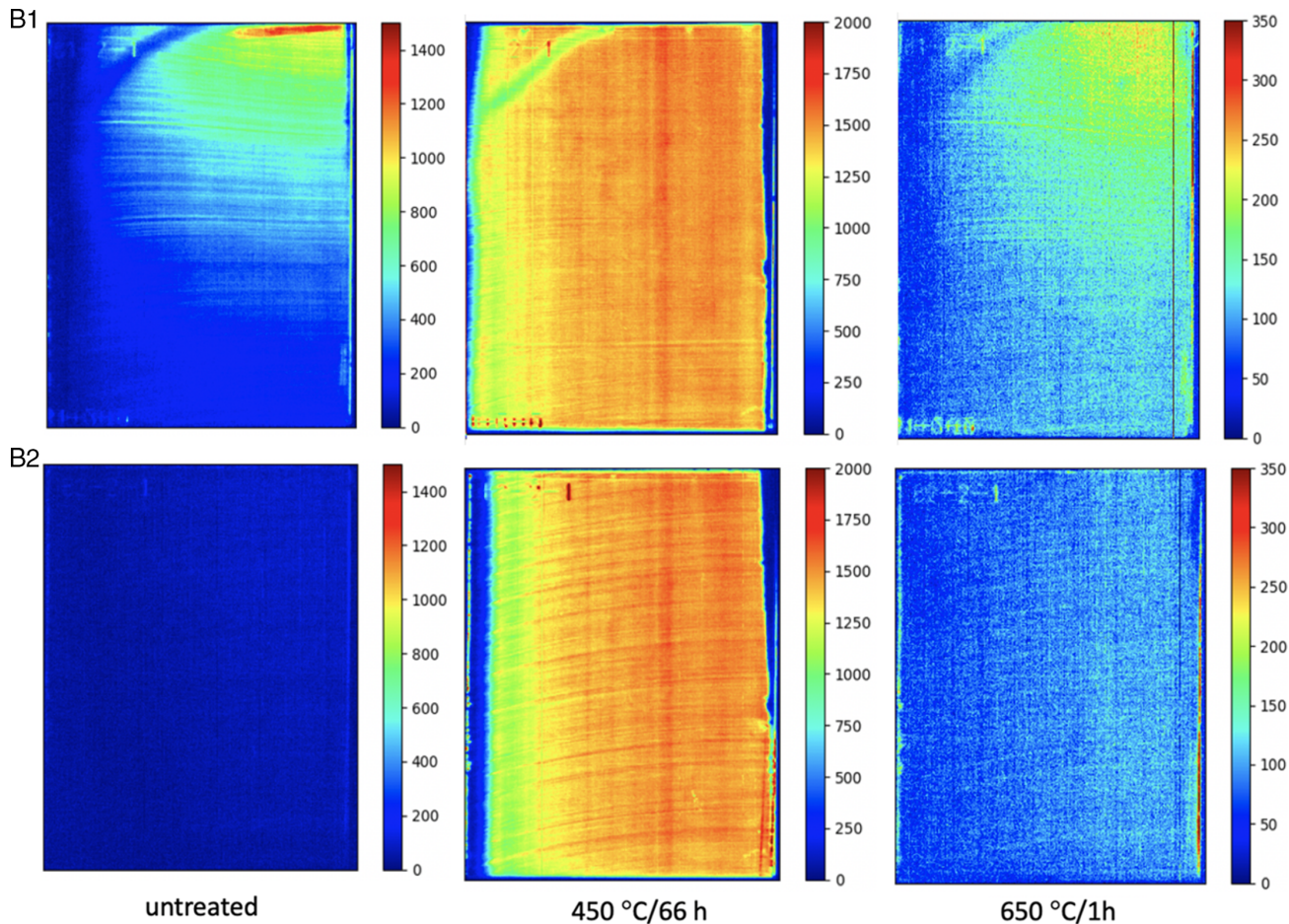


Figure 16. The development in the spatial distribution of the P-line (0.767 eV) PL emission in crystal B (1.3 mm min^{-1}) before and after thermal treatment at $450\text{ }^{\circ}\text{C}$ and $650\text{ }^{\circ}\text{C}$.

Two ingots have been studied where samples have been cut from the seed end as well as further down in the ingot. The ingots were manufactured with different pulling speeds and had different levels of oxygen incorporated in the crystals. FTIR spectroscopy measurements confirmed that the slowly pulled crystal exhibited higher levels of O_i than the crystal pulled more rapidly. The integrated spectra from the samples showed characteristic emissions associated with TDs with the highest levels found toward the seed end in the slowly pulled crystal. The band-to-band emission which is related to the lifetime of photogenerated charge carriers and the TD-associated emission were inversely related. Heat treatment at $450\text{ }^{\circ}\text{C}$ for 66 h seemed to form TDs in the samples, where these were not formed during manufacturing. In the slowly pulled crystal, TDs seemed to have formed to their full extent in the seed end material during manufacture, while the material further down in the ingot exhibited less such formation. The rapidly pulled crystal only exhibited minor TD-associated luminescence after production. A higher pull speed during crystal manufacturing seems to be an effective way of both reducing the O_i levels and diminishing the formation of TDs in Cz-Si during crystal pulling. However, thermal treatment of this at $450\text{ }^{\circ}\text{C}$ led to the formation of TDs to a similar extent as in the slowly pulled crystal. After TD formation, the band-to-band PL emission

was significantly lower, suggesting a drastic decrease in the lifetime of excited charge carriers. Further treatment at $650\text{ }^{\circ}\text{C}$ for 1 h removed the TD-related PL signal effectively in the chemically polished, etched samples, boosting the BB signal to substantially higher levels than in the untreated material. Thus, thermal treatment at $650\text{ }^{\circ}\text{C}$ is a potential method for upgrading Cz-Si with excessive TD levels.

The unetched, as-cut samples developed a broad emission peak previously reported on as-cut horizontal wafers after treatment at $650\text{ }^{\circ}\text{C}$. This was not experienced with the etched samples, leading to the conclusion that this was a surface-related phenomenon.

Acknowledgements

This work was performed as a part of the FME-SuSolTech research center, sponsored by the Norwegian Research Council, in cooperation with industrial partners (contract: 257639/E20). It is further based on H. Stalheims' M.Sc. thesis.

Conflict of Interest

The authors declare no conflict of interest.

Data Availability Statement

The data that support the findings of this study are available from the corresponding author upon reasonable request.

Keywords

Cz-ingots, hyperspectral imaging, pull speeds, spectroscopy, thermal donors

Received: September 28, 2021

Revised: October 21, 2021

Published online: November 17, 2021

-
- [1] C. S. Fuller, R. A. Logan, *J. Appl. Phys.* **1957**, *28*, 1427.
 - [2] J. D. Murphy, M. Al-Amin, K. Bothe, M. Olmo, V. V. Voronkov, R. J. Falster, *J. Appl. Phys.* **2015**, *118*, 12.
 - [3] J. D. Murphy, K. Bothe, R. Krain, V. V. Voronkov, R. J. Falster, *J. Appl. Phys.* **2012**, *111*, 10.
 - [4] J. Schon, T. Niewelt, D. Mu, S. Maus, A. Wolf, J. D. Murphy, M. C. Schubert, *IEEE J. Photovolt.* **2021**, *11*, 289.
 - [5] J. Veirman, S. Dubois, N. Enjalbert, J. P. Garandet, D. R. Heslinga, M. Lemiti, *Solid-State Electron.* **2010**, *54*, 671.
 - [6] W. Kaiser, H. L. Frisch, H. Reiss, *Phys. Rev.* **1958**, *112*, 1546.
 - [7] R. C. Newman, *J. Phys. Condens. Matter* **2000**, *12*, R335.
 - [8] P. Wagner, J. Hage, *Appl. Phys. A: Mater. Sci. Process.* **1989**, *49*, 123.
 - [9] R. Singh, P. B. Nagabalsubramanian, in *Proc. of the 3rd Int. Conf. on Condensed Matter and Applied Physics* AIP publishing, Bikaner, India (Eds.: M. S. Shekhawat, S. Bhardwaj, B. Suthar), **2020**.
 - [10] K. Torigoe, T. Ono, *AIP Adv.* **2020**, *10*, 045019.
 - [11] R. Basnet, H. Sio, M. Siriwardhana, F. E. Rougier, D. Macdonald, *Phys. Status Solidi A-Appl. Mater. Sci.* **2021**, *218*, 2000587.
 - [12] Y. Matsushita, *J. Cryst. Growth* **1982**, *56*, 516.
 - [13] H. Nakanishi, H. Kohda, K. Hoshikawa, *J. Cryst. Growth* **1983**, *61*, 80.
 - [14] T. Niewelt, S. Lim, J. Holtkamp, J. Schon, W. Warta, D. Macdonald, M. C. Schubert, *Sol. Energ. Mat. Sol. C* **2014**, *131*, 117.
 - [15] J. Haunschmid, I. E. Reis, J. Geilker, S. Rein, *Phys. Status Solidi-R* **2011**, *5*, 199.
 - [16] R. Basnet, C. Sun, H. T. Wu, H. T. Nguyen, F. E. Rougier, D. Macdonald, *J. Appl. Phys.* **2018**, *124*, 7.
 - [17] H. Angelskar, R. Sondena, M. S. Wiig, E. S. Marstein, *Characterization of Oxidation-Induced Stacking Fault Rings in Cz Silicon: Photoluminescence Imaging and Visual Inspection after Wright Etch*. *Energy Procedia*, Elsevier Science Bv, IMEC, Leuven, Belgium **2012**, p. 160.
 - [18] E. Olsen, M. I. Helander, T. Mehl, I. Burud, *Phys. Status Solidi A-Appl. Mater. Sci.* **2020**, *217*, 190084.
 - [19] N. S. Minaev, A. V. Mudryi, *Physica Status Solidi (a)* **1981**, *68*, 561.
 - [20] M. Tajima, Y. Ishikawa, H. Kiuchi, A. Ogura, *Appl. Phys. Express* **2018**, *11*, 041301.
 - [21] E. Olsen, A. S. Flo, *Appl. Phys. Lett.* **2011**, *99*, 011903.
 - [22] I. Burud, T. Mehl, A. Flo, D. Lausch, E. Olsen, *J. Spectr. Imaging* **2016**, *5*, a8.
 - [23] Y. Hu, H. Schon, E. J. Ovrelied, O. Nielsen, L. Arnberg, *AIP Adv.* **2012**, *2*, 8.
 - [24] M. I. Helander, *Thermal Donors in Czochralski Silicon Wafers Investigated by Spectral Imaging [MSc]*. NMBU, Ås, Norway **2018**.
 - [25] R. Sondena, Y. Hu, M. Juel, M. S. Wiig, H. Angelskar, *J. Cryst. Growth* **2013**, *367*, 68.
 - [26] G. Coletti, P. Manshanden, S. Bernardini, P. C. P. Bronsveld, A. Gutjahr, Z. Hu, G. Li, *Sol. Energ. Mat. Sol. C* **2014**, *130*, 647.
 - [27] V. V. Voronkov, R. Falster, in *Gettering and Defect Engineering in Semiconductor Technology* Trans Tech Publications, Loipersdorf, Austria (Eds.: W. Jantsch, F. Schaffler) **2011**, p. XIV.
 - [28] Y. Hu, H. Schon, O. Nielsen, E. J. Ovrelied, L. Arnberg, *J. Appl. Phys.* **2012**, *111*, 053101.
 - [29] J. Haunschmid, J. Broisch, I. Reis, S. Rein, in *Proc. of the 26th EUPVSEC*, WIP, Munchen, Hamburg, Germany **2011**, p. 1025.
 - [30] C. Claeys, E. Simoen, J. Vanhellemont, *J. Phys. III* **1997**, *7*, 1469.